

Understanding Radio Irregularity in Wireless Networks

Torsten Muetze Patrick Stuedi Fabian Kuhn Gustavo Alonso
Swiss Federal Institute of Technology (ETHZ)
Department of Computer Science
8092 Zurich, Switzerland
{torsten.muetze, stuedip, kuhn, alonso}@inf.ethz.ch

Abstract—In an effort to better understand connectivity and capacity in wireless networks, the log-normal shadowing radio propagation model is used to capture radio irregularities and obstacles in the transmission path. Existing results indicate that log-normal shadowing results in higher connectivity and interference levels as shadowing (i.e., the radio irregularity) increases. In this paper we demonstrate that such a behavior is mainly caused by an unnatural bias of the log-normal shadowing radio propagation model that results in a larger transmission range as shadowing increases. To avoid this effect, we analyze connectivity and interference under log-normal shadowing using a normalization that compensates for the enlarged radio transmission range. Our analysis shows that log-normal shadowing still improves the connectivity of a wireless network and even reduces interference. We explain this behavior by studying in detail what network parameters are affected by shadowing. Our results indicate that, when it comes to connectivity and interference, an analysis based on a circular transmission range leads to worst case results.

I. INTRODUCTION

Understanding connectivity and radio interference in wireless networks is an important step to determine their overall throughput capacity. In an effort to overcome the limitations of the deterministic path loss model (where the transmission range is a perfect circle), connectivity ([4], [1], [7], [6], [12]) and capacity ([10], [11]) have recently been studied in the context of the log-normal shadowing radio propagation model [9], [14]. In this model, the radio irregularity can be controlled through a single parameter: the shadowing deviation. As the shadowing deviation grows, the transmission range turns into a more irregular shape, mirroring what happens in reality with antennas that are not ideal (not perfectly isotropic) and obstacles that cut the transmission range short in a given direction.

In this paper, we use the log-normal shadowing radio propagation model to explore the impact of radio irregularity on connectivity and interference in a wireless network. We show that the log-normal shadowing model introduces an unnatural bias into the analysis: as the shadowing deviation grows, the radio transmission range not only becomes more irregular, but also enlarges. This naturally leads to an improved connectivity. At the same time, the enlarged transmission range leads to an increase in interference. These are results already mentioned

The work presented in this paper was supported (in part) by the National Competence Center in Research on Mobile Information and Communication Systems (NCCR-MICS), a center supported by the Swiss National Science Foundation under grant number 5005-67322.

in the literature [1], [6], [12], [11]. The problem is, however, that the increase in transmission range does not correspond to any real phenomenon [3]. Intuitively speaking, increasing the irregularity by adding obstructions to the transmission path should not generally improve the perceived signal quality.

The main objective of this paper is therefore to obtain an unbiased view on the effects of radio irregularity on connectivity and interference in a wireless network. We propose a method to eliminate the bias introduced by the log-normal shadowing model. This allows us to capture the intrinsic properties of radio irregularity and thus to compare different levels of irregularity in a meaningful way. Our approach compensates for the enlarged radio transmission range by adjusting the transmission power of the nodes accordingly. This technique is also used in percolation theory when comparing different network models [8], [2], [5]. Interestingly, when using this technique, connectivity still increases and interference even decreases as the radio propagation becomes more irregular.

Overall, these results are an important contribution since, when taken together, they show that an analysis of connectivity and interference in a circular radio propagation model yields worst case bounds for both connectivity and interference. Until now, the assumption that shadowing increased interference led to assuming that a circular radio propagation range was a best case scenario for network capacity.

The paper is structured as follows: Section II describes the network model we use. Effects of radio irregularity on properties of the network graph like connectivity, node degree and the distribution of the edge length are described in Section III. In Section IV we obtain expressions for the cumulated noise and the number of interfering nodes per network link and discuss how radio irregularity affects interference. Section V concludes the paper.

II. NETWORK MODEL

A. Deployment Area

We consider a set of n nodes uniformly distributed on a square area of side length λ , $\Lambda_\lambda := \frac{1}{2}[-\lambda, \lambda]^2$. The number of nodes on every subarea $\Omega \subseteq \Lambda_\lambda$ follows a binomial distribution with success probability $|\Omega|/\lambda^2$. Keeping the node density $\mu := n/\lambda^2$ constant and letting $\lambda \rightarrow \infty$ yields an infinite deployment area $\Lambda_\infty = \mathbb{R}^2$, where the number of nodes on every subarea Ω is Poisson distributed with expectation $\mu|\Omega|$. While in a real-world scenario or a computer simulation

TABLE I
FREQUENTLY USED SYMBOLS.

$\Lambda_\lambda = \frac{1}{2}[-\lambda, \lambda]^2$	Node deployment area
n	Number of nodes
$\mu = n/\lambda^2$	Node density
p_0	Transmission power
r_0	Antenna far-field reference distance
ϱ	Path loss exponent
$\beta \cdot p^*$	Threshold power for radio reception (threshold constant β , ambient noise power p^*)
r_t	Threshold distance
X ($\mathbb{E}[X] = 0, \text{Var}[X] = \sigma^2$)	Normal distributed shadowing random variable
P (or $P_{a \leftarrow b}$)	Reception power (at node a when sending from node b)
R	Distance between two randomly chosen nodes
$\varphi : \mathbb{R}_{\geq 0} \rightarrow [0, 1]$ $\varphi(r) = \Pr[P \geq \beta p^* R = r]$	Connection function
$N_{\leftrightarrow}, N_{\rightrightarrows}$	Number of neighbors of a node in the symmetric and asymmetric link model

the deployment area is always finite, analytical calculations are often considerably simplified by working on $\Lambda_\infty = \mathbb{R}^2$, thereby avoiding boundary conditions. In the paper we always indicate when a finite and when an infinite deployment area is considered. We explore to which extent results for the infinite case carry over to the finite setting by computer simulations. To suppress boundary effects in a simulation we calculate the quantity in question only over a scope — a square subarea centered in the deployment area — and indicate the size of the scope in the legend or caption of the corresponding figure.

B. Connection Function

Which node pairs can establish a direct communication link is determined by the *connection function* $\varphi : \mathbb{R}_{\geq 0} \rightarrow [0, 1]$ — the probability that a signal can be received correctly in distance r from a sender node is given by $\varphi(r)$. The connection function can be derived from the radio propagation model (the radio propagation models and connection functions we consider in the paper are direction invariant). In the *symmetric link model* the signal path between two nodes is assumed to behave identical in either direction, whereas in the *asymmetric link model* the properties of the signal path are assumed to depend on the direction of transmission. Thus, two nodes in distance r are connected by an undirected edge in the network graph with probability $\varphi(r)$ in the symmetric link model (one coin is tossed for every pair of nodes) or with probability $\varphi(r)^2$ in the asymmetric link model (two coins are tossed for every pair of nodes).

C. Radio Propagation Model

In the paper we use the *log-normal shadowing* radio propagation model (LNS) and assume all nodes use the same signal power (see [9], [3] for experimental evidence, and [4], [1], [7], [6], [12], [10], [11] for related work using the same model). In the log-normal shadowing model, the reception power in distance $R = r$ from a node transmitting with signal power

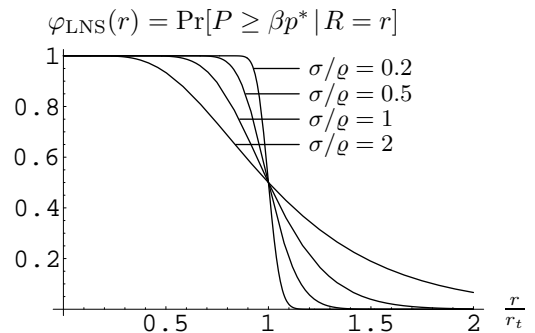


Fig. 1. Connection function for log-normal shadowing.

p_0 is a random variable defined by

$$P = p_0 \left(\frac{r_0}{r} \right)^\varrho 10^{X/10}, \quad (1)$$

with $r_0 > 0$ being the *reference distance for the antenna far-field*, $\varrho > 0$ the *path loss exponent*, and X a normal distributed random variable with zero mean and standard deviation σ (referred to as the *shadowing deviation*).¹ If the shadowing deviation is equal to zero ($\sigma = 0$), the radio propagation range is a perfect circle (this is also called the *deterministic path loss model*). As the shadowing deviation grows, the shape of the transmission range becomes more random and irregular. In particular, the larger the shadowing deviation, the more likely distant nodes gain connection and nearby nodes lose connection.

We define the *threshold distance* as the distance where the received signal power, when $\sigma = 0$, drops to some threshold value $\beta \cdot p^* < p_0$, where β is the *threshold constant* and p^* the *ambient noise power*. The threshold distance is given by

$$r_t = r_0 \left(\frac{p_0}{\beta p^*} \right)^{1/\varrho}. \quad (2)$$

From (1), the connection function for the log-normal shadowing radio propagation model calculates as²

$$\begin{aligned} \varphi_{\text{LNS}}(r) &= \Pr[P \geq \beta p^* | R = r] = \Pr \left[X \geq \frac{10\varrho \ln(r/r_t)}{\ln(10)} \right] \\ &= \frac{1}{2} - \frac{1}{2} \operatorname{erf} \left(\frac{10\varrho \ln(r/r_t)}{\sqrt{2} \ln(10) \sigma} \right). \end{aligned} \quad (3)$$

Fig. 1 plots the connection probability for log-normal shadowing versus the node distance. The function is shown for different values of the shadowing deviation normalized to the path loss exponent (σ/ϱ), as the shape depends only on this ratio. For small values of σ/ϱ , the connection function becomes a step function and the resulting network graph a unit disk graph with disks of radius $r/r_t = 1$.

¹From a physical point of view the received signal power never exceeds the transmitted power. Hence, (1) can hold only for $r > r_0$, while for $r \leq r_0$ the definition $P = p_0$ should be adopted. However, numerically this distinction rarely makes a significant difference, the only time we have to take it into account is in Theorem 10 where otherwise integrals would not converge.

²The error function is defined for all real numbers x as $\operatorname{erf}(x) := \frac{2}{\sqrt{\pi}} \int_0^x \exp(-t^2) dt$.

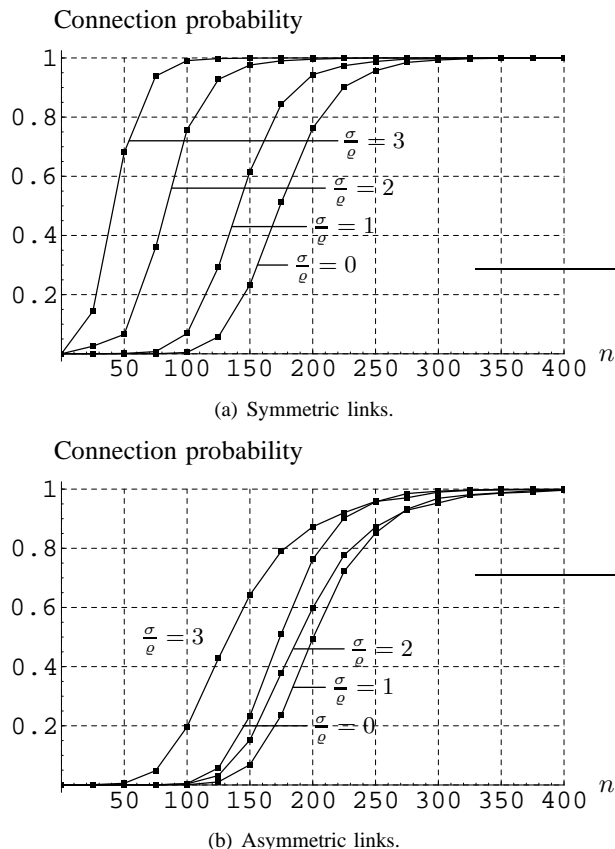


Fig. 2. Connectivity under log-normal shadowing (simulations on $\Lambda_{2000} = [-1000, 1000]^2$ in scope $[-500, 500]^2$, $\rho = 4$, $r_t = 200$).

In this paper, we focus on the log-normal shadowing radio propagation model. However, we want to emphasize that the concept of connection function we use is powerful enough to capture other probabilistic radio propagation models and effects, e.g. Rayleigh fading [6, Sect. II-E] or uniform fluctuation of the transmission power p_0 in (1). For this reason, throughout the paper we first state our results for an arbitrary connection function and then consider the special case of log-normal shadowing.

III. IMPACT OF SHADOWING ON CONNECTIVITY

In this section we demonstrate that using the standard log-normal shadowing model to study connectivity leads to an undesired effect. The positive impact of the shadowing deviation on connectivity is first and foremost caused by a bias towards an enlarged radio transmission range in the model, rather than by an intrinsic property of radio irregularity (Section III-A). This is the result of the shadowing deviation inducing unrealistic power levels which in turn affect the node degree (i.e., the number of neighbors of a given node). To eliminate this effect, we adapt the transmission power of the nodes such that the expected node degree remains constant with respect to the shadowing deviation. We want to emphasize that this should not be seen as a criticism of the log-normal shadowing model in general. Instead, we introduce a natural normalization

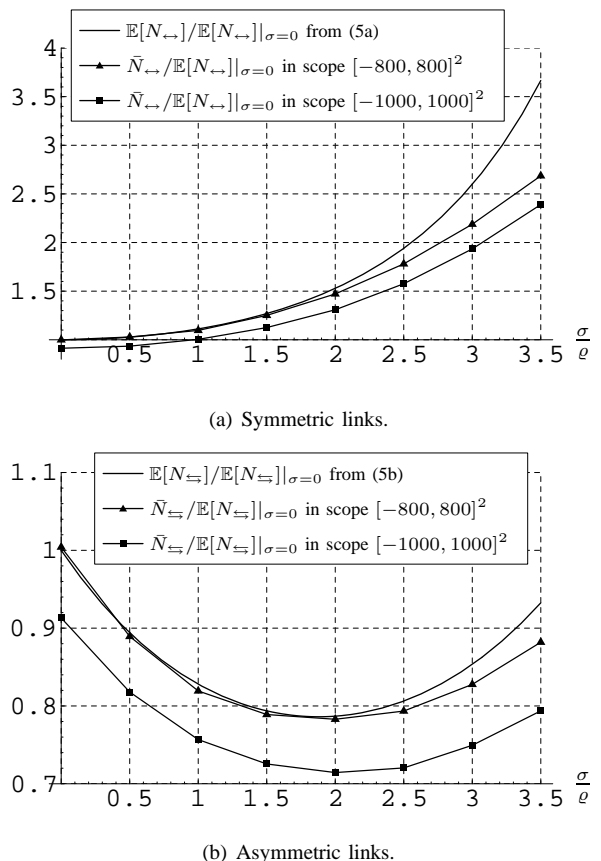


Fig. 3. Expected node degree under log-normal shadowing (simulations on $\Lambda_{2000} = [-1000, 1000]^2$, $n = 200$, $\rho = 4$, $r_t = 200$).

that allows a fair comparison of the connectivity in different settings as the shadowing deviation changes (Section III-B). Note that the same technique is commonly used in percolation theory when comparing the connectivity in different network models [8], [2], [5].

Our results show that connectivity increases with shadowing even when the expected node degree is kept constant. We explain this phenomenon by showing that the connectivity improvement is the result of shadowing increasing the average length of the network graph edges (Section III-C).

A. Connectivity in the Standard LNS Model

To study how connectivity evolves with an increasing shadowing deviation, we performed a number of simulations measuring the probability of the network graph to be connected as a function of the node density (we consider only the subgraph within a scope, but connecting paths may contain intermediate nodes outside of it). We plot the probability for different values of the shadowing deviation normalized to the path loss exponent (σ/ρ). Fig. 2(a) shows connectivity in the symmetric link model, and Fig. 2(b) for asymmetric links. For symmetric links shadowing improves the connectivity (as observed in [1]). For asymmetric links connectivity decreases as the normalized shadowing deviation grows from 0 to 1 (as shown in [12]). Connectivity increases as the normalized

shadowing deviation grows further to 2 and 3. We are not aware that this has been observed before.

We can explain this somewhat counterintuitive behavior through the following theorem (extending results from [7, Sect. III] and [6, Sect. II-D], where only symmetric links are considered).

Theorem 1. *Let N_{\leftrightarrow} and N_{\rightleftharpoons} be random variables denoting the number of neighbors of a node in the symmetric and asymmetric link model, respectively.*

On $\Lambda_\infty = \mathbb{R}^2$ both N_{\leftrightarrow} and N_{\rightleftharpoons} are Poisson distributed with expectations

$$\mathbb{E}[N_{\leftrightarrow}] = \mu 2\pi \int_0^\infty r\varphi(r)dr \quad (4a)$$

$$\mathbb{E}[N_{\rightleftharpoons}] = \mu 2\pi \int_0^\infty r\varphi(r)^2dr. \quad (4b)$$

For the log-normal shadowing connection function (3) these integrals evaluate to

$$\mathbb{E}[N_{\leftrightarrow}] = \mu\pi r_t^2 \exp\left(2\left(\frac{\ln(10)\sigma}{10\varrho}\right)^2\right) \geq \mu\pi r_t^2 \quad (5a)$$

$$\mathbb{E}[N_{\rightleftharpoons}] = \mu\pi r_t^2 \exp\left(2\left(\frac{\ln(10)\sigma}{10\varrho}\right)^2\right) \left(1 - \operatorname{erf}\left(\frac{\ln(10)\sigma}{10\varrho}\right)\right). \quad (5b)$$

Proof. The number of nodes in an annulus of width dr and radius r is Poisson distributed with expectation $\mu 2\pi r dr$. The number of neighbors in this annulus is Poisson distributed with expectation $\mu 2\pi r \varphi(r) dr$ for symmetric links and $\mu 2\pi r \varphi(r)^2 dr$ for asymmetric links. The sum of independent Poisson distributed random variables is Poisson distributed. \square

The expressions (5a) and (5b) quantify how the expected node degree depends on the shadowing deviation. In Fig. 3 we plot the expected node degree calculated from these expressions and compare it to simulation results. We do this for the symmetric (Fig. 3(a)) and the asymmetric link model (Fig. 3(b)). The figures indicate that the simulation results match very well the analytical expressions. They also illustrate the boundary effects: the results from simulations considering the whole deployment area differ quantitatively from those restricted to a smaller scope (as nodes close to the boundary have less neighbors). Most importantly, the figures capture the bias introduced by the log-normal shadowing radio propagation model: the expected node degree changes with the shadowing deviation. In the symmetric link model, the increase in node degree as shadowing increases naturally improves connectivity. This explains the connectivity increase shown in Fig. 2(a). In the asymmetric link model, the expected node degree first decreases for $0 \leq \sigma/\varrho \leq 1.88$, it increases again for $\sigma/\varrho > 1.88$. This explains the counterintuitive behavior of connectivity observed in Fig. 2(b).

These results show that log-normal shadowing primarily affects the node degree, which in turn affects connectivity. This is because an increasing shadowing deviation results not only in a more irregular, but also in an enlarged radio transmission range, which is an unnatural side effect of the log-normal shadowing radio propagation model. In what follows, we avoid this effect by adjusting the transmission power

of the nodes such that the expected node degree is kept constant for different values of the shadowing deviation. To give some geometric intuition, this is equivalent to keeping the transmission area always the same regardless of the shape (and thus equal to a circle area for $\sigma = 0$).

B. Connectivity Under Constant Node Degree

Based on the above observation, we adjust the transmission power of every node as a function of the shadowing deviation, such that the expected node degree remains constant and equal to that when the shadowing deviation is zero. We can easily compute the required power values from (5a) and (5b) as follows.

Corollary 2. *In the log-normal shadowing radio propagation model on $\Lambda_\infty = \mathbb{R}^2$, the transmission powers p_{\leftrightarrow} and p_{\rightleftharpoons} such that*

$$\mathbb{E}[N_{\leftrightarrow}]|_{p_0=p_{\leftrightarrow}} = \mathbb{E}[N_{\leftrightarrow}]|_{\sigma=0} \quad (6a)$$

$$\mathbb{E}[N_{\rightleftharpoons}]|_{p_0=p_{\rightleftharpoons}} = \mathbb{E}[N_{\rightleftharpoons}]|_{\sigma=0} \quad (6b)$$

are

$$p_{\leftrightarrow} = p_0 \exp\left(-\frac{\ln(10)\sigma^2}{100\varrho}\right) \quad (7a)$$

$$p_{\rightleftharpoons} = p_0 \exp\left(-\frac{\ln(10)\sigma^2}{100\varrho}\right) \left(1 - \operatorname{erf}\left(\frac{\ln(10)\sigma}{10\varrho}\right)\right)^{-\frac{6}{2}}. \quad (7b)$$

In Fig. 4 we show how connectivity evolves with the shadowing deviation, this time using the transmission powers (7) that preserve the expected node degree. Again, we consider both the symmetric (Fig. 4(a)) and the asymmetric link model (Fig. 4(b)).

Our simulation results demonstrate that *connectivity increases with the shadowing deviation both for symmetric and asymmetric links, if the expected node degree is kept constant*. To the best of our knowledge this is the first result capturing the intrinsic impact of radio irregularity on connectivity under log-normal shadowing. In the next section we discover a plausible reason for the observed phenomenon: an increasing average edge length. Before we come to this, let us briefly put our approach into a wider context.

The results of [8] and [2] from percolation theory [5] indicate an improved connectivity if the connection function gets spread out, while keeping the expected node degree constant. Note, however, that these authors apply a different normalization scheme: Using the symmetric link model they consider a family of connection functions

$$\left(\frac{1}{t}\varphi\left(\frac{1}{\sqrt{t}}\bullet\right)\right)_{t>0} \quad (8a)$$

for an increasing parameter t . In the asymmetric link model this corresponds to a family of functions

$$\left(\frac{1}{t}\varphi\left(\frac{1}{t}\bullet\right)\right)_{t>0}. \quad (8b)$$

In contrast to that we consider the function families

$$\left(\varphi_{\text{LNS}}(\bullet)\right)_{p_0=p_{\leftrightarrow}}_{\sigma>0} \quad (9a)$$

$$\left(\varphi_{\text{LNS}}(\bullet)\right)_{p_0=p_{\rightleftharpoons}}_{\sigma>0} \quad (9b)$$

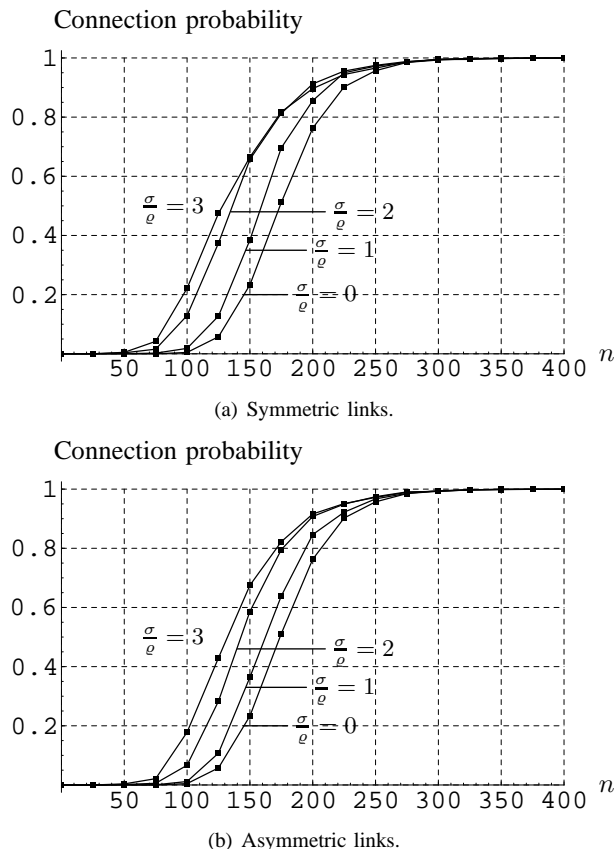


Fig. 4. Connectivity under log-normal shadowing using the transmission powers (7) that preserve the expected node degree (simulations on $\Lambda_{2000} = [-1000, 1000]^2$ in scope $[-500, 500]^2$, $\varrho = 4$, $r_t = 200$).

for an increasing shadowing deviation σ .

As we will show in the following, the increase in the average edge length holds for both normalization schemes (8) and (9).

C. Impact of Shadowing on Edge Length

To explore why connectivity increases with the shadowing deviation, even when the node degree is kept constant, we study the distributions of distance and reception power between a randomly chosen pair of nodes (chosen either among all pairs of nodes or pairs that are connected by an edge in the network graph), yielding the edge length distribution of the network graph. In Theorem 7 and Corollary 8 we prove that the average edge length increases with the shadowing deviation (under constant node degree). The results on the power distribution will also be used in Section IV when dealing with interference. Unless specified otherwise, we assume links to be symmetric throughout this section. Nevertheless, our results apply similarly to the case of asymmetric links.³

1) *Distance and Power Distribution*: Starting point for our derivation is the well-known distance distribution for random

³If instead of symmetric links the asymmetric link model shall be used, every occurrence of $f_{P|R=r}(p)$ and every occurrence of $\varphi(r)$ in (14), (15), (16) and (17) has to be replaced by $\varphi(r)f_{P|R=r}(p)$ and $\varphi(r)^2$, respectively. All other results, in particular (18), remain unchanged.

square line picking [13].⁴

Consider the following experiment on a finite deployment area $\Lambda_\lambda = \frac{1}{2}[-\lambda, \lambda]^2$: Choose a pair of nodes at random and denote by R and P the distance and the reception power between the two nodes.

Lemma 3 (M. Trott [13]). *The probability density function of R is*

$$f_R(r) = \begin{cases} \frac{2r}{\lambda^2} \left(\frac{r^2}{\lambda^2} - 4\frac{r}{\lambda} + \pi \right) & 0 \leq r \leq \lambda \\ \frac{2r}{\lambda^2} \left(4\sqrt{\frac{r^2}{\lambda^2} - 1} - \left(\frac{r^2}{\lambda^2} + 2 \right) - \pi \right) & \lambda \leq r \leq \sqrt{2}\lambda \\ 0 & \text{otherwise.} \end{cases} \quad (10)$$

The node distance relates to the reception power via the radio propagation model. The following lemma relies on basic conditional probability laws and is stated without a proof.

Lemma 4. *With the conditional density $f_{P|R=r}$ as a property of the radio propagation model, the joint density $f_{R,P}$ and the density f_P can be calculated as*

$$f_{R,P}(r, p) = f_R(r) f_{P|R=r}(p) \quad (11)$$

$$f_P(p) = \int_0^{\sqrt{2}\lambda} f_{R,P}(r, p) dr. \quad (12)$$

In the log-normal shadowing radio propagation model, the reception power P is log-normal distributed for a fixed distance $R = r$ (cp. (1)):

$$f_{P|R=r}(p) = \frac{10}{\ln(10)\sqrt{2\pi p\sigma}} \exp\left(-\frac{50(\ln(\frac{p}{p_0}(\frac{r}{r_0})^\varrho))^2}{(\ln(10)\sigma)^2}\right). \quad (13)$$

2) *Edge Length Distribution*: Now consider the following modified experiment: Randomly choose a pair of nodes *that are connected by an edge* (recall, that we assume links to be symmetric throughout this section) and denote by R' and P' the distance and the reception power between the two nodes.

Theorem 5. *The joint probability density function of R' and P' is*

$$f_{R',P'}(r, p) = \begin{cases} \frac{f_R(r)f_{P|R=r}(p)}{\int_0^{\sqrt{2}\lambda} f_R(r)\varphi(r)dr} & p \geq \beta p^* \\ 0 & \text{otherwise.} \end{cases} \quad (14)$$

For $\lambda \rightarrow \infty$ we have

$$f_{R',P'}(r, p) = \begin{cases} \frac{r f_{P|R=r}(p)}{\int_0^\infty r \varphi(r) dr} & p \geq \beta p^* \\ 0 & \text{otherwise,} \end{cases} \quad (15)$$

provided that the integral in the denominator exists.

Proof. The joint density $f_{R',P'}$ can be obtained from $f_{R,P}$ by conditioning on $P \geq \beta p^*$ and using the relation $\int_{\beta p^*}^\infty f_{P|R=r}(p) dp = \Pr[P \geq \beta p^* | R = r] = \varphi(r)$. The distance density can be written as $f_R(r) = \frac{1}{\lambda} (2\pi \frac{r}{\lambda} + \mathcal{O}((\frac{r}{\lambda})^2))$ for $\lambda \rightarrow \infty$. Plugging this into (14) yields (15). \square

⁴Note that all results in this section remain valid, e.g. for a rectangular or circular deployment area, only the distance density function for square line picking has to be replaced by the density function for the respective shape.

Corollary 6. *The probability density function of R' is*

$$f_{R'}(r) = \frac{f_R(r)\varphi(r)}{\int_0^{\sqrt{2}\lambda} f_R(r)\varphi(r)dr}. \quad (16)$$

For $\lambda \rightarrow \infty$ we have

$$f_{R'}(r) = \frac{r\varphi(r)}{\int_0^\infty r\varphi(r)dr}, \quad (17)$$

provided that the integral in the denominator exists. For a step function $\varphi = 1_{[0, r_t]}$ ($r_t > 0$) it does exist and R' follows a triangular distribution:

$$f_{R'}(r) = \begin{cases} 2\frac{r}{r_t^2} & 0 \leq r \leq r_t \\ 0 & \text{otherwise.} \end{cases} \quad (18)$$

Proof. The first two claims follow by plugging (14) and (15) into $f_{R'}(r) = \int_0^\infty f_{R', P'}(r, p)dp$. Then (18) follows by straightforward calculation. \square

Corollary 6 shows that the edge length of the network graph under log-normal shadowing approximately follows a triangular distribution if $\sigma/\rho \ll 1$ and $r_t \ll \lambda$.^{5 6}

3) *Shadowing Increases the Edge Length:* The following theorem is a very general statement about the edge length of network graphs resulting from two different connection functions.

Theorem 7. *Let φ_1 and φ_2 be connection functions that satisfy the relations*

$$\int_0^\infty r\varphi_1(r)dr = \int_0^\infty r\varphi_2(r)dr \quad (19a)$$

$$\bigwedge_{x \geq 0} \int_x^\infty r\varphi_1(r)dr \geq \int_x^\infty r\varphi_2(r)dr, \quad (19b)$$

and for which $\int_0^\infty r^2\varphi_1(r)dr$ and $\int_0^\infty r^2\varphi_2(r)dr$ are finite. Then the average edge lengths $\mathbb{E}[R'_1]$ and $\mathbb{E}[R'_2]$ of the network graphs on $\Lambda_\infty = \mathbb{R}^2$ in the symmetric link model resulting from φ_1 and φ_2 , respectively, satisfy

$$\mathbb{E}[R'_1] \geq \mathbb{E}[R'_2]. \quad (20)$$

Proof. By plugging (17) into $\mathbb{E}[R'] = \int_0^\infty r f_{R'}(r)dr$ and using the abbreviation $\psi(r) := r(\varphi_1(r) - \varphi_2(r))$ we observe that it suffices to show that for all $x \geq 0$

$$\int_x^\infty \psi(r)dr \geq 0 \implies \int_x^\infty r\psi(r)dr \geq 0. \quad (21)$$

For $x \geq 0$ we define $\Psi(x) := \int_x^\infty \psi(r)dr$ and use integration by parts (note that $\int \psi(r)dr = -\Psi(r) + c$ for some $c \in \mathbb{R}$):

$$\int_x^\infty r\psi(r)dr = x\Psi(x) - \lim_{r \rightarrow \infty} r\Psi(r) + \int_x^\infty \Psi(r)dr. \quad (22)$$

If we could show that $\lim_{r \rightarrow \infty} r\Psi(r) = 0$ this would imply the theorem since $\Psi(x)$ is non-negative by assumption.

⁵Corollary 6 also corrects a result from [7, Sect. II] on the edge length distribution under log-normal shadowing on an infinite deployment area. The authors obtain a different density than we get when plugging (3) into (17).

⁶Analogously to the approach in Corollary 6 one can easily derive the distribution of the edge power P' from Theorem 5. Since this distribution is not of interest for the rest of the paper, we omit these calculations.

For $\tilde{r} \geq 0$ we have $\tilde{r}\varphi_i(\tilde{r}) \geq 0$ ($i = 1, 2$), therefore

$$\lim_{r \rightarrow \infty} r \int_r^\infty \tilde{r}\varphi_i(\tilde{r})d\tilde{r} \geq 0 \quad (23)$$

$$\lim_{r \rightarrow \infty} r \int_r^\infty \tilde{r}\varphi_i(\tilde{r})d\tilde{r} \leq \lim_{r \rightarrow \infty} \int_r^\infty \tilde{r}^2\varphi_i(\tilde{r})d\tilde{r} = 0. \quad (24)$$

This implies $\lim_{r \rightarrow \infty} r \int_r^\infty \tilde{r}\varphi_i(\tilde{r})d\tilde{r} = 0$ ($i = 1, 2$), which in turn yields $\lim_{r \rightarrow \infty} r\Psi(r) = 0$. \square

Note that Theorem 7 extends to the asymmetric link model by substituting φ_1^2 for φ_1 and φ_2^2 for φ_2 .

Condition (19a) expresses that φ_1 and φ_2 generate the same expected node degree (cp. (4a)), and (19b) formalizes that φ_1 generates more distant and less nearby neighbors than φ_2 .

Theorem 7 applies to the connection function for log-normal shadowing when using the transmission powers (7). We leave it to the reader to check that

$$\varphi_i := \varphi_{\text{LNS}}|_{\substack{p_0=p_{\leftrightarrow} \\ \sigma=\sigma_i}} \quad (i = 1, 2) \quad (25)$$

indeed satisfy (19) provided that $\sigma_1 > \sigma_2$. The same holds for

$$\varphi_i := \varphi_{\text{LNS}}^2|_{\substack{p_0=p_{\Leftarrow} \\ \sigma=\sigma_i}} \quad (i = 1, 2). \quad (26)$$

Hence, the average edge length increases with the shadowing deviation σ . Theorem 7 can also be employed to show that the normalization scheme (8) increases the average edge length. As condition (19) applies to both normalization schemes (8) and (9) so nicely, it seems to capture the heart of our problem in a natural way.⁷

The following corollary determines the predicted edge length increase under log-normal shadowing precisely, and thereby justifies the positive effect of an increasing shadowing deviation on connectivity.⁸

Corollary 8. *Consider the log-normal shadowing radio propagation model on $\Lambda_\infty = \mathbb{R}^2$ using the transmission powers (7) that preserve the expected node degree.*

The average length of the network graph edges in the symmetric and asymmetric link model is

$$\mathbb{E}[R'_{\leftrightarrow}]|_{p_0=p_{\leftrightarrow}} = \frac{2}{3}r_t \exp\left(\frac{3}{2}\left(\frac{\ln(10)\sigma}{10\rho}\right)^2\right) \quad (27)$$

$$\mathbb{E}[R'_{\Leftarrow}]|_{p_0=p_{\Leftarrow}} = \frac{2}{3}r_t \exp\left(\frac{3}{2}\left(\frac{\ln(10)\sigma}{10\rho}\right)^2\right) \frac{(1 - \operatorname{erf}\left(\frac{3}{2}\frac{\ln(10)\sigma}{10\rho}\right))}{(1 - \operatorname{erf}\left(\frac{\ln(10)\sigma}{10\rho}\right))^{\frac{3}{2}}}. \quad (28)$$

Both terms are strictly increasing with σ .

Proof. The result for symmetric links follows by successively plugging (17), (3), (2) and finally (7a) into $\mathbb{E}[R'] = \int_0^\infty r f_{R'}(r)dr$. The calculation for asymmetric links proceeds similarly, only replace $\varphi(r)$ in (17) by $\varphi(r)^2$ and use (7b) instead of (7a). \square

⁷An interesting open question with respect to connectivity is the relation between the critical node densities μ_1 and μ_2 for percolation in network graphs on $\Lambda_\infty = \mathbb{R}^2$ based on connection functions φ_1 and φ_2 , respectively (at the critical node density an infinite network graph component appears with probability one). The aim would be to prove or disprove that condition (19) implies $\mu_1 \leq \mu_2$.

⁸For the normalization scheme (8), the precise edge length increase can be determined similarly, a calculation we omit due to the limited space.

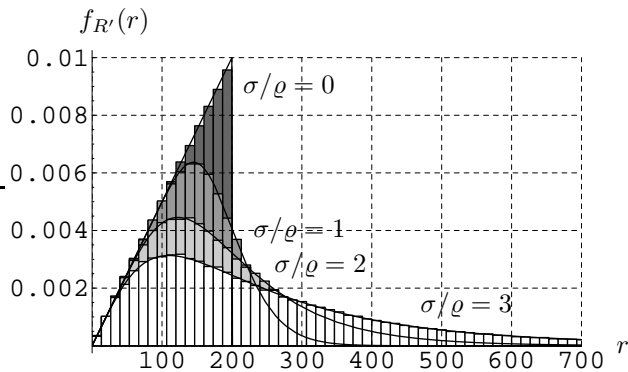


Fig. 5. Edge length distribution under log-normal shadowing when using the transmission power from (7a) (analytical curves from (17), histograms from simulations on $\Lambda_{16000} = [-8000, 8000]^2$, $n = 12800$, $\varrho = 4$, $r_t = 200$).

In Fig. 5 we plot the edge length distribution (17) for different values of the shadowing deviation and compare it to simulation results (be reminded that they are based on the transmission power (7a) that preserves the expected node degree). As can be observed, the analytical curves match very well the simulation results. The figure also illustrates how the edge length distribution spreads out with shadowing and increasingly deviates from a triangular distribution. This causes the average edge length to increase as predicted by Corollary 8. The increase in the average edge length justifies the connectivity improvement caused by radio irregularity as observed in the previous section.

Our results indicate that — contrary to what intuition might suggest — radio irregularity is indeed beneficial for network connectivity.

IV. IMPACT OF SHADOWING ON INTERFERENCE

Throughput capacity is another important property of wireless networks. As with connectivity, it is difficult to find closed expressions for the capacity of a wireless network, and even more complicated to analytically study the effects of log-normal shadowing on capacity. In [10], it is shown that the capacity of a network is mainly limited by interference (to be more precise, by the number of interfering nodes per network link). In this section we try to gain a quantitative understanding of interference under log-normal shadowing.

We first describe the signal-to-interference-plus-noise-ratio model (SINR) and calculate expressions for the number of interfering nodes per network link (Section IV-A). We then demonstrate that the impact of the shadowing deviation on interference is mainly caused by a bias towards an enlarged transmission range in the radio propagation model (Section IV-B). We compensate for this effect by adjusting the transmission power of the nodes such that the expected cumulated noise remains constant with respect to the shadowing deviation (Section IV-C).

Our results show that interference decreases with shadowing when the expected cumulated noise is kept constant. We explain this phenomenon by showing that the interference

reduction is caused by a spread of the power distribution under shadowing.

A. The SINR Model

In the *signal-to-interference-plus-noise-ratio model* (SINR), a signal from node b can be decoded correctly at node a , if

$$p_{a \leftarrow b} \geq \beta \left(p^* + \underbrace{\sum_{b' \in \bar{I}} p_{a \leftarrow b'}}_{=: p_{\bar{I}}} \right) \quad (29)$$

holds, where $\bar{I} \subseteq N \setminus \{a, b\}$ is the subset of nodes transmitting concurrently with b . Note that (29) with $\bar{I} = \emptyset$ is necessary for two nodes to be connected by an edge in the network graph. A smallest set of nodes I such that $\bar{I} = N \setminus (I \cup \{a, b\})$ satisfies (29) is called a *set of interferers* (w.r.t. the transmission from node b to node a with reception power $p_{a \leftarrow b}$); the interfering nodes from I must not transmit concurrently with node b , while the *non-interferers* from \bar{I} may do so. The size of a set of interferers is uniquely determined and referred to as the *number of interferers*.

A set of interferers can easily be determined by sorting the received signal powers $(p_{a \leftarrow b'})_{b' \in N \setminus \{a, b\}}$ and successively adding nodes to the set \bar{I} , starting with those that contribute the lowest signal powers, as long as (29) is satisfied. Then $I := (N \setminus \{a, b\}) \setminus \bar{I}$ is a set of interferers. For the deterministic path loss model (i.e., log-normal shadowing with $\sigma = 0$) sorting the nodes according to signal power and sorting according to distance from node a induces the same node order. In this case interferers and non-interferers can be separated by a circle centered at node a .

Reusing results from Section III-C (recall the definitions of R , P , R' and P'), the following theorem determines the expected number of interferers for an arbitrary radio propagation model, in particular for log-normal shadowing.

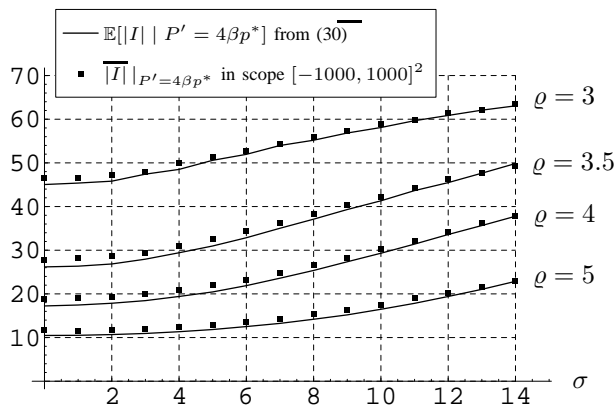
Theorem 9. *On $\Lambda_\lambda = \frac{1}{2}[-\lambda, \lambda]^2$ the expected number of interferers for a transmission from node b to node a with power $p_{a \leftarrow b} =: p \geq \beta p^*$ equals*

$$\mathbb{E}[|I| \mid P' = p] = (n - 2) \int_\tau^\infty f_P(\tilde{p}) d\tilde{p}, \quad (30)$$

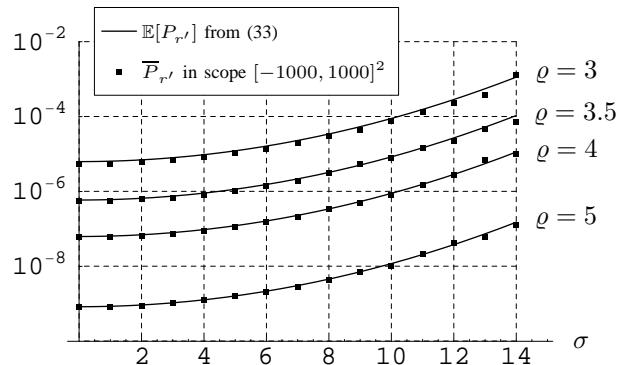
where τ is a solution of the equation

$$(n - 2) \int_0^\tau \tilde{p} f_P(\tilde{p}) d\tilde{p} = \frac{p}{\beta} - p^*. \quad (31)$$

Proof. From (29) we obtain the maximum admissible noise for a transmission from node b to node a as $p_{\bar{I}} = p/\beta - p^*$. The number of nodes from which node a receives a signal in the range $[\tilde{p}, \tilde{p} + d\tilde{p}]$ is $(n - 2) f_P(\tilde{p}) d\tilde{p}$, the noise from these nodes is $(n - 2) \tilde{p} f_P(\tilde{p}) d\tilde{p}$. Interferers are nodes from which node a receives the highest signal powers, while non-interferers are nodes from which node a receives the lowest signal powers (the latter may transmit concurrently with node b , the former must not). Equating the maximum admissible noise with the cumulated noise from the non-interferers yields (31). Suppose this equation has two solutions τ and τ' . Since



(a) Expected number of interferers under log-normal shadowing (simulations on $\Lambda_{2000} = [-1000, 1000]^2$, $n = 200$, $p_0 = 1$, $r_0 = 1$, $\beta = 2.5$, $r_t = 200$).



(b) Expected cumulated noise from outside a circle of radius $r' = 50$ under log-normal shadowing (simulations on $\Lambda_{2000} = [-1000, 1000]^2$, $n = 200$, $p_0 = 1$, $r_0 = 1$).

Fig. 6. Interference increase as a side effect of log-normal shadowing.

$\int_{\tau}^{\tau'} \tilde{p} f_P(\tilde{p}) d\tilde{p} = 0$ implies $\int_{\tau}^{\tau'} f_P(\tilde{p}) d\tilde{p} = 0$ the right hand side of (30) is well-defined. \square

The price for the generality of Theorem 9 is, that the integrals (30) and (31) can only be treated numerically, in particular since f_P itself is given by another integral (12).

B. Interference in the Standard LNS Model

To study how interference evolves with an increasing shadowing deviation, we plot in Fig. 6(a) the expected number of interferers versus the shadowing deviation, with the path loss exponent as a parameter. The expected number of interferers obtained from (30) and the simulation results match very well. The figure also shows that shadowing increases the number of interfering nodes.

We can explain this behavior by calculating the expected cumulated noise perceived at a given node, as formalized in the following theorem.

Theorem 10. Let $P_{r'}$ be a random variable denoting the cumulated received signal power from all nodes in a distance at least r' from a receiver node.

On $\Lambda_{\infty} = \mathbb{R}^2$ the expectation of $P_{r'}$ is

$$\mathbb{E}[P_{r'}] = \mu 2\pi \int_{r'}^{\infty} r \mathbb{E}[P | R = r] dr. \quad (32)$$

For the log-normal shadowing radio propagation model with $\varrho > 2$ this integral evaluates to

$$\mathbb{E}[P_{r'}] = \begin{cases} p_0 \mu \pi \left(r_0^2 \left(\frac{2}{\varrho-2} \exp\left(\frac{(\ln(10)\sigma)^2}{200}\right) + 1 \right) - r'^2 \right) & r' \leq r_0 \\ \frac{2 p_0 \mu \pi r_0^{\varrho} \exp\left(\frac{(\ln(10)\sigma)^2}{200}\right)}{r'^{\varrho-2} (\varrho-2)} & r' \geq r_0. \end{cases} \quad (33)$$

Proof. The proof of (32) resembles that of (4).

For the log-normal shadowing model we obtain from (1)

$$\mathbb{E}[P | R = r] = p_0 \left(\frac{r_0}{r}\right)^{\varrho} \exp\left(\frac{(\ln(10)\sigma)^2}{200}\right) \quad (34)$$

for $r > r_0$ and $\mathbb{E}[P | R = r] = p_0$ for $r \leq r_0$ (we distinguish between $r > r_0$ and $r \leq r_0$ here, if otherwise (34) was used

for all $r \geq 0$ the integral $\int_0^{\infty} r \mathbb{E}[P | R = r] dr$ would not converge). Plugging this into (32) yields the result. \square

In Fig. 6(b) we plot the expected cumulated noise from outside a circle of radius $r' = 50$ versus the shadowing deviation. The expected noise calculated from (33) and the simulation results show excellent agreement. Most importantly, the figure illustrates that the expected cumulated noise increases with the shadowing deviation. This is a side effect of the log-normal shadowing radio propagation model enlarging the transmission range as the shadowing deviation grows. Since interference in the SINR model is primarily affected by the cumulated noise, the increase in the number of interferers is not surprising. Therefore, to study the impact of radio irregularity on interference in a meaningful way, it is reasonable to adjust the power levels such that the expected cumulated noise is preserved. This resembles our approach from Section III where we studied connectivity under constant expected node degree.

C. Interference Under Constant Noise

Based on the above observation, we adjust the transmission power as a function of the shadowing deviation, such that the expected cumulated noise remains constant and equal to that when the shadowing deviation is zero. We can easily compute the required power values from (33) as follows.

Corollary 11. In the log-normal shadowing radio propagation model with $\varrho > 2$ on $\Lambda_{\infty} = \mathbb{R}^2$, the transmission power p_{\sim} such that

$$\mathbb{E}[P_{r'}]_{p_0=p_{\sim}} = \mathbb{E}[P_{r'}]_{\sigma=0} \quad (35)$$

holds for $r' \geq r_0$ is

$$p_{\sim} = p_0 \exp\left(-\frac{(\ln(10)\sigma)^2}{200}\right). \quad (36)$$

In Fig. 7 we plot the expected number of interferers versus the shadowing deviation, with the path loss exponent as a parameter. Here we employ the transmission power from (36). Again, we compare the expected number of interferers

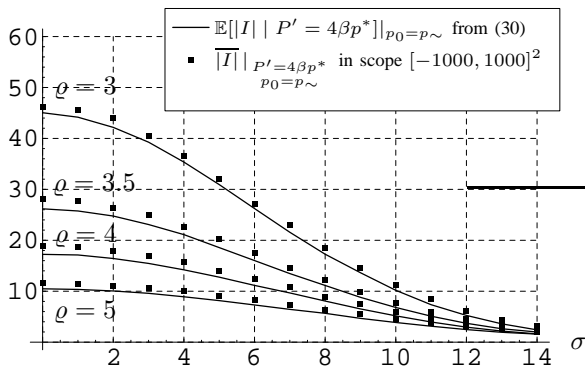


Fig. 7. Expected number of interferers under log-normal shadowing using the transmission power (36) that preserves the expected cumulated noise (simulations on $\Lambda_{2000} = [-1000, 1000]^2$, $n = 200$, $p_0 = 1$, $r_0 = 1$, $\beta = 2.5$, $r_t = 200$).

obtained from (30) to simulation results and find very good agreement. In contrast to Fig. 6(a) we observe that the number of interferers no longer increases, but decreases as the shadowing deviation grows.

This phenomenon can be explained as follows: an increasing shadowing deviation spreads out the power density function f_P , increasing both the number of node pairs with a low reception power and those with a high reception power (balanced such that the cumulated noise remains constant). Consequently, it takes more nodes to reach the maximum admissible noise $p_{\bar{I}}$ (cp. (29)) — nodes that qualify as non-interferers. Hence the number of interferers decreases. Fig. 8 shows the power distribution for different values of the shadowing deviation. As can be observed, low reception powers become more likely as the shadowing deviation grows. The same holds for high reception powers, but this is not depicted in the figure to maintain its clarity.

To the best of our knowledge this is the first result capturing the intrinsic impact of radio irregularity on interference under log-normal shadowing. Our results indicate that radio irregularity is not only beneficial for connectivity but also for interference.

An interesting open question is how radio-irregularity impacts other factors apart from interference that influence the throughput capacity of a wireless network (route length, edge usage), and finally to address capacity itself. One difficulty here is to define a reasonable measure of comparability for the radio-irregularity induced by log-normal shadowing, since capacity is affected by graph-theoretic (route length, edge usage) and non-graph-theoretic properties (SINR interference).

V. CONCLUSION

In this paper we have studied the impact of log-normal shadowing on connectivity and interference in a wireless network. Unlike previous work, where results are distorted by an artifact of the log-normal shadowing radio propagation model, we employ a method that allows a fair comparison among different levels of radio irregularity. We have shown

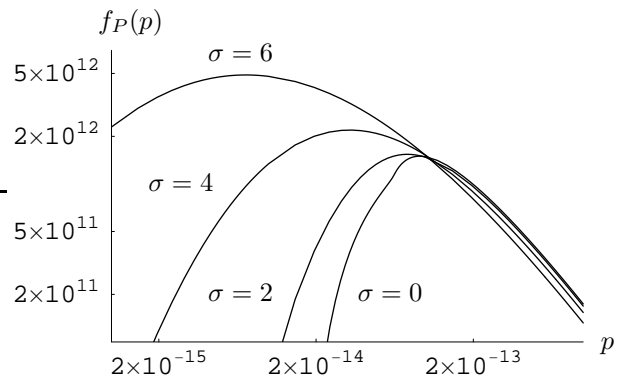


Fig. 8. Power distribution under log-normal shadowing when using the transmission power (36) that preserves the expected cumulated noise (analytical curves from (12), $\Lambda_{2000} = [-1000, 1000]^2$, $p_0 = 1$, $r_0 = 1$, $\rho = 4$).

that under a reasonable measure of comparability log-normal shadowing improves the connectivity of a network and reduces interference. Our results illustrate that the radio irregularity induced by log-normal shadowing has indeed a beneficial impact on connectivity and interference. This is of interest for many existing bounds on the connectivity and throughput capacity of wireless networks that have been derived using the deterministic path loss model, as our results indicate these are lower instead of upper bounds on connectivity and capacity.

REFERENCES

- [1] C. Bettstetter and C. Hartmann. Connectivity of wireless multihop networks in a shadow fading environment. *Wireless Networks*, 11:571–579, Sept. 2005.
- [2] L. Booth, J. Bruck, M. Cook, and M. Franceschetti. Ad hoc wireless networks with noisy links. In *Proc. IEEE International Symposium on Information Theory (ISIT)*, page 386, Yokohama, Japan, June 2003.
- [3] D. C. Cox, R. Murray, and A. Norris. 800 MHz attenuation measured in and around suburban houses. *AT&T Bell Lab. Tech. J.*, 63(6):921–954, 1984.
- [4] R. Hekmat and P. V. Mieghem. Connectivity in wireless ad-hoc networks with a log-normal radio model. *Mobile Networks and Applications*, 11:351–360, 2006.
- [5] R. Meester and R. Roy. *Continuum Percolation*. Cambridge University Press, 1996.
- [6] D. Miorandi and E. Altman. Coverage and connectivity of ad hoc networks in presence of channel randomness. In *Proc. IEEE 24th Annual Joint Conference of the IEEE Computer and Communications Societies (INFOCOM)*, pages 491–502, Mar. 2005.
- [7] J. Orriss and S. K. Barton. Probability distributions for the number of radio transceivers which can communicate with one another. *IEEE Trans. Commun.*, 51(4):676–681, 2003.
- [8] M. D. Penrose. On the spread-out limit for bond and continuum percolation. *Ann. Appl. Probab.*, 3(1):253–276, 1993.
- [9] T. S. Rappaport. *Wireless Communications: Principles & Practice*, chapter 4.9.2. Prentice Hall, second edition, 2002.
- [10] P. Stuedi and G. Alonso. Computing throughput capacity for realistic wireless multihop networks. In *Proc. ACM International Symposium on Modeling Analysis and Simulation of Wireless and Mobile Systems*, pages 191–198, 2006.
- [11] P. Stuedi and G. Alonso. Log-normal shadowing meets SINR: A numerical study of capacity in wireless networks. In *Proc. IEEE Sensor Mesh and Ad Hoc Communications and Networks (SECON)*, June 2007.
- [12] P. Stuedi, O. Chinellato, and G. Alonso. Connectivity in the presence of shadowing in 802.11 ad hoc networks. In *Proc. IEEE Wireless Communications and Networking Conference (WCNC)*, pages 2225–2230, Mar. 2005.

- [13] M. Trott. The Mathematica Guidebooks additional material: Average distance distribution, 2004.
- [14] D. Tse and P. Viswanath. *Fundamentals of Wireless Communication*, chapter 2.1.6. Cambridge University Press, 2005.